

HOSTED BY



Contents lists available at ScienceDirect

The Egyptian Journal of Remote Sensing and Space Sciences

journal homepage: www.sciencedirect.com

The contribution of CurvaTool semi-automatic approach in structural and groundwater investigations. A case study in the Main Ethiopian Rift Valley

Sabrina Bonetto^a, Anna Facello^b, Gessica Umili^{a,*}

^a Department of Earth Sciences, University of Turin, via Valperga Caluso 35, 10125 Turin, Italy

^b TriM (Translate into Meaning), srl. Corso Sommeiller 24, 10128 Turin, Italy

ARTICLE INFO

Article history:

Received 5 March 2018

Revised 14 September 2018

Accepted 18 October 2018

Available online 10 December 2018

Keywords:

MER
CurvaTool
SRTM
Groundwater
Lineaments

ABSTRACT

In this study, a semi-automatic approach implemented in the code CurvaTool has been applied to the analysis of the structural asset and its potential relationship with local water distribution in an area of the central sector of the Main Ethiopian Rift Valley. A 30 m SRTM DEM was used as input for CurvaTool code. A first processing was performed over the whole area (about 10,640 km²). Subsequently, a second processing was carried out over a smaller portion of the original DEM, in order to analyze in detail its morphological and structural features. CurvaTool output data show three main linear feature sets, characterized by non-homogeneous distributions, which have been validated by morphological and geological literature data. Concerning the hydrogeological framework, the analysis of water points distribution shows alignments coherent with the trends of linear features extracted by CurvaTool. This correspondence might suggest a structural control on the groundwater flow paths of the analyzed area and highlight the utility of the semi-automatic CurvaTool approach in the preliminary phase of an hydrogeological study in areas where groundwater flow is conditioned by topography and morphotectonic asset, particularly in case of fractured basement aquifer systems in region with lack of geological information or reduced accessibility.

© 2018 National Authority for Remote Sensing and Space Sciences. Production and hosting by Elsevier B.V. This is an open access article under the CC BY-NC-ND license (<http://creativecommons.org/licenses/by-nc-nd/4.0/>).

1. Introduction

Groundwater plays an important role in supplying water for human consumption, agriculture, livestock and economic activities and it contributes to improve economic and health conditions in areas of arid and hyper-arid environments (Luczaj, 2016). In many African countries the freshwater demand is arising due to the decrease of precipitation and the increase of population; therefore, groundwater exploration is a challenge, particularly in consideration of the complex hydrogeology and low potential yields of many semiarid zones (Magaia et al., 2017). Geology of those areas is mainly constituted by crystalline rocks of the basement that are usually characterized by a secondary porosity connected with the presence and interconnection of fractures, faults and shear zones,

which represent a favorable settings for hosting and channeling groundwater (Sultan et al., 2008; Tessema et al., 2012).

On this subject, the knowledge of the structural asset provides information on the dynamics of groundwater resources that flow along preferred pathways connected to tectonic lineaments. In particular, several studies revealed a close relationship between (i) lineaments, groundwater flow and yield (Mabee et al., 1994; Magowe and Carr, 1999; Fernandes and Rudolph, 2001), (ii) groundwater productivity and number of lineaments or lineament density, rather than lineaments themselves (Prabu and Rajagopalan, 2013). Therefore, lineaments trend and distribution may be essential in groundwater surveys, development and management.

Traditional field investigations in African countries are often inadequate for climatic conditions, accessibility and security, particularly in case of extended areas to be explored. In recent years, aerial techniques based on satellite imageries and aerial photographs have been used for investigating groundwater aquifers, opening a new research field in applied geology (Corgne et al., 2010; Assatse et al., 2016; Adewumi, 2016).

Peer review under responsibility of National Authority for Remote Sensing and Space Sciences.

* Corresponding author.

E-mail addresses: sabrina.bonetto@unito.it (S. Bonetto), gessica.umili@unito.it (G. Umili).

<https://doi.org/10.1016/j.ejrs.2018.10.003>

1110-9823/© 2018 National Authority for Remote Sensing and Space Sciences. Production and hosting by Elsevier B.V. This is an open access article under the CC BY-NC-ND license (<http://creativecommons.org/licenses/by-nc-nd/4.0/>).

Aerial photographs, remotely sensed images and digital terrain/elevation models have been already used in groundwater investigations (Edet et al., 1998; El-Naqa et al., 2009; Obiefuna et al., 2010; Anudu et al., 2011; Elewa and Qaddah, 2011; Mogaji et al., 2011; Talab and Tijani, 2011; Phukon et al., 2012; Chuma et al., 2013; Okereke et al., 2015; Yenne et al., 2015; Adewumi, 2016). Recently, the availability of several satellite data and the improvement of image processing techniques have enlarged the potential of remote sensing data and their products in delineating the geological structures with better accuracy (Masoud and Koike, 2006; Akame et al., 2014). Other techniques were also applied to emphasize the role of remote sensing in detecting lineaments (Corgne et al., 2010; Jacques et al., 2012; Rashid et al., 2012; Singh et al., 2013; Assatse et al., 2016; Bonetto et al., 2015b, 2017).

The authors propose the use of remotely sensed models in combination with a semi-automatic approach for linear features identification and extraction (CurvaTool) in ground-based hydrogeological surveys for a better understanding of the role of structural elements in local water distribution. In particular, CurvaTool was used for the analysis of a 30 m SRTM DEM of an area of the central sector of the Main Ethiopian Rift Valley (MER), in order to (i) produce a map of the spatial distribution of morphological linear features, (ii) identify the structural trends with a fast, cheap and semi-automatic method and (iii) evaluate the potential structural controls on groundwater flow and wells distribution. Output data of the code were compared and validated with literature information, geological maps and hydrogeological fieldworks data.

2. Geological and hydrogeological setting

MER is a seismically and volcanically active portion of the East African Rift System. It trends along a NNE-SSW direction and it is bordered by Ethiopian Plateau to W and Somali Plateau to E (Benvenuti et al., 2002). MER has been traditionally divided into three sectors based on surface geology and geomorphology: (i) the northern (NMER), from the Afar depression to near Lake Koka, (ii) the central (CMER), from Lake Koka through the lakes region to Lake Awasa, and (iii) the southern (SMER) sector, from Lake Awasa into the broadly rifted zone of southern Ethiopia (Keranen and Klemperer, 2008).

The study area is located in CMER and, in particular, in the Zway-Shala basin, which includes Zway, Abjata, Langano and Shala Lakes (Fig. 1).

CMER mainly consists of volcanic products (pyroclastic rocks, rhyolites, tuffs and basaltic lava flows) (Abebe et al., 1998; Boccaletti et al., 1999; Benvenuti et al., 2002; Ayenew, 2008) and sediment deposits (volcano-lacustrine and fluvio-lacustrine deposits) that cover large areas of the lowlands (Boccaletti et al., 1998; Benvenuti et al., 2002; Rango et al., 2010; Abbate et al., 2015) (Fig. 2).

MER is divided into three physiographic zones: rift, transitional escarpments and highlands; it is characterized by the presence of many lakes, most of them originated when volcanoes stopped their activity and their evolution was marked by alternate transgressive and regressive phases. In particular, Ziway, Langano, Abijata, Awasa and Shala Lakes are located in CMER and are remnants of

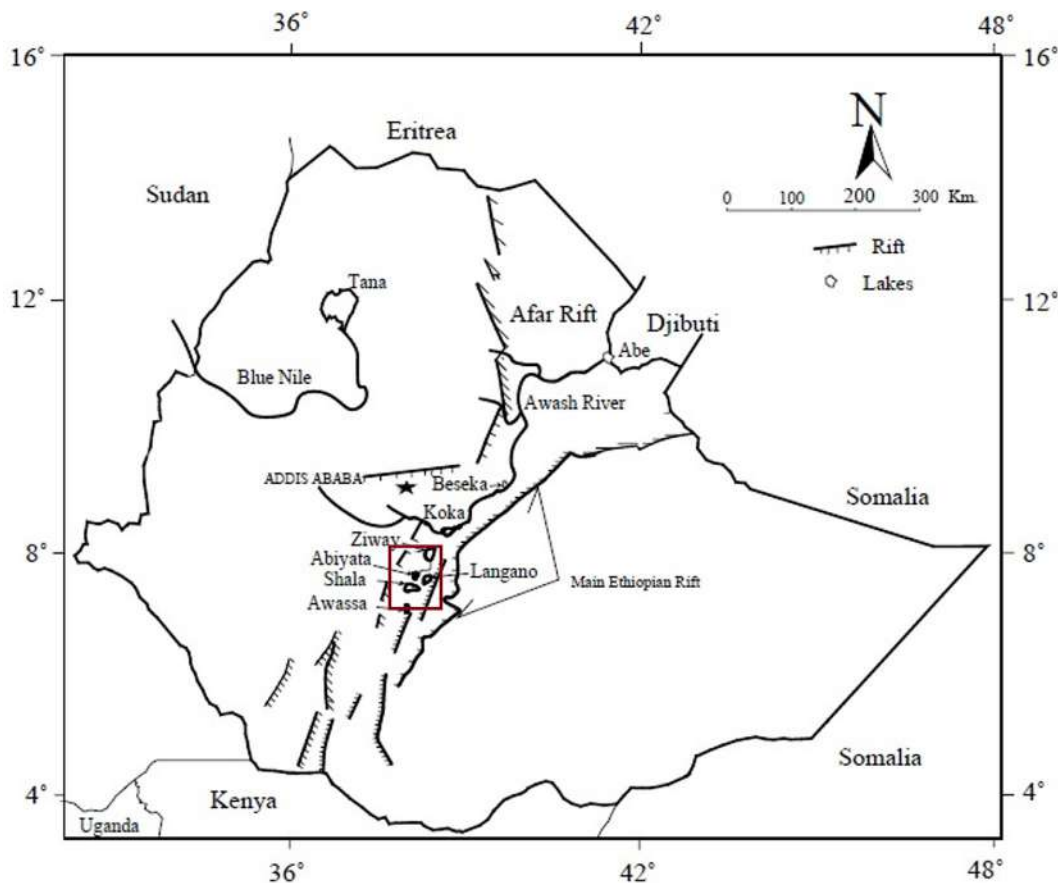


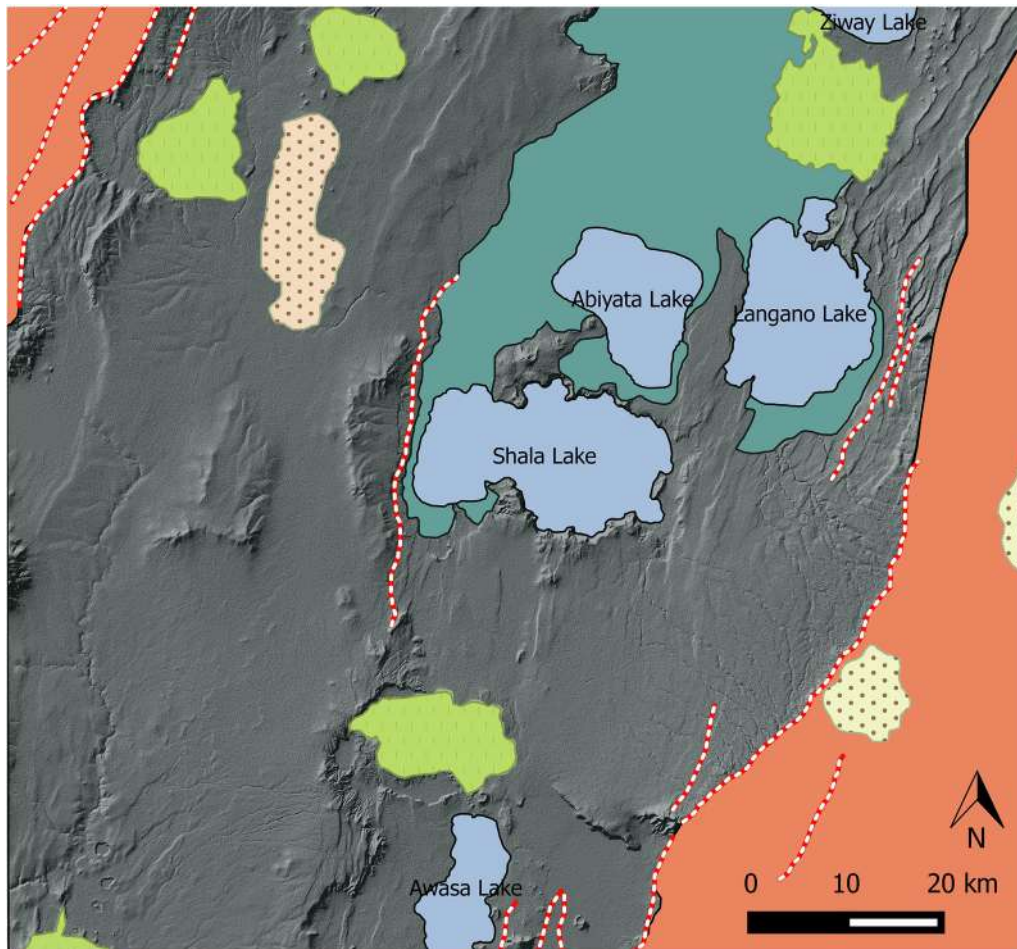
Fig. 1. Location of the Main Ethiopian Rift; red frame includes the study area (modified after Bonetto et al., 2016).

a much larger lake basin that reached its maximum size during Late Pleistocene and Early Holocene (Benvenuti et al., 2002).

MER is characterized by extensional tectonics and, generally, faults are parallel and sub-parallel to the NE–SW trending rift axis (Fig. 3). There are at least three sets of faults trending NNE–SSW, N–S, NNW–SSE, in addition to curved volcanic vent structures. The first two sets are dominant and extend for long distances, following the axis of a tectonically active fault system called Wonji Fault Belt (WFB) (Boccaletti et al., 1999; Abbate et al., 2015). The marginal escarpments have well-defined steep normal fault scarps (Ayenew et al., 2008). An E–W to NW–SE trending cross-rift oblique-slip transfer faults system is also reported. In the highlands different sets of faults are reported, representing older structural trends (Ayenew et al., 2008; Benvenuti et al., 2002).

According to EIGS (1993), in MER two major aquifer classes can be identified: (i) extensive aquifers with intergranular permeability (unconsolidated sediments: alluvium, eluvium, colluvium and lacustrine sediments) and (ii) extensively fractured and weathered volcanics (basalts, rhyolites, trachytes and ignimbrites).

Considering the different morphological domains, the rift floor is characterized both by fractured basaltic and ignimbritic aquifers, which are mainly unconfined and leaky types, and permeable alluvial and colluvial deposits associated with lacustrine soils forming the main shallow aquifers. Conversely, in the highlands, multi-layer confined, semi-confined (leaky) and unconfined aquifers are very common: both alluvial deposits and weathered volcanics with limited interbedded alluvial gravels and sands are present.



Geology



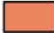

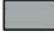



- | | | | |
|---|---|--|------------|
|  | Lacustrine, fluvial and colluvial deposits |  | Main Fault |
|  | Volcanites of the plateau |  | Lakes |
|  | Rift floor ignimbrites | | |
|  | Rhyolitic lava flow | | |
|  | Basaltic lava flows and scoria cones | | |
|  | Basalts, mugearites, trachytes and phonolites | | |

Fig. 2. Simplified geological map of the study area, according to literature data (modified after Boccaletti et al., 1998; Rango et al., 2010).

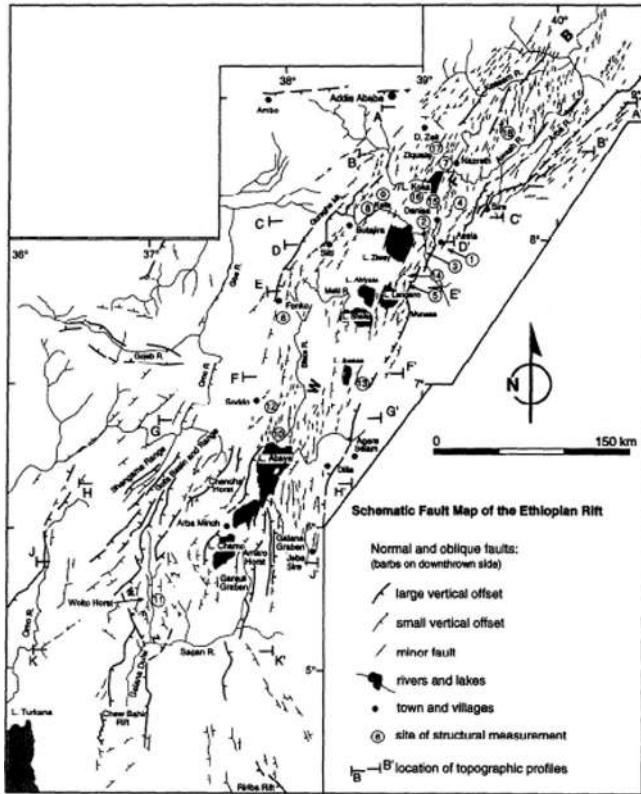


Fig. 3. Schematic structural map of MER based on field satellite (Landsat) observations (Source Boccaletti et al., 1998).

3. Methodology

In 2009, a census of 67 water points (wells and springs) was performed in the Zway-Shala basin (Bonetto et al., 2015a). According to the digging process, wells were classified into deep drilled wells (ranging from 20 to 400 m deep) and shallow hand-dug wells (up to 20 m deep). In detail, 16 shallow hand-dug wells, 30 deep drilled wells and 21 springs were analyzed.

Faults have significantly increased rocks permeability of this area, with particular regard to volcanic rocks, in which the flow is dominantly fault-controlled. Considering the potential role of the faults in the dynamics of the subsurface fluid flow and the direct knowledge of most of the water points in the studied area, this work aims to verify this connection by applying a fast and cheap semi-automatic method (CurvaTool) to detect tectonic trend and lineament zones that could influence water distribution.

Curvatool code is used to process a 30 m SRTM v3 (raster data format, source USGS EROS Data Center (EDC), <https://lta.cr.usgs.gov/SRTM>) for rapidly identifying linear features and detecting their main trends. Results are compared with geological literature data and geographical distribution of the censused water points, in order to validate the reliability of the method for structural and hydrogeological studies.

4. Data processing

CurvaTool (Umili et al., 2013) is a semi-automatic code for linear features identification and extraction on a DEM representing a portion of territory: it is based on the assumption that a geological

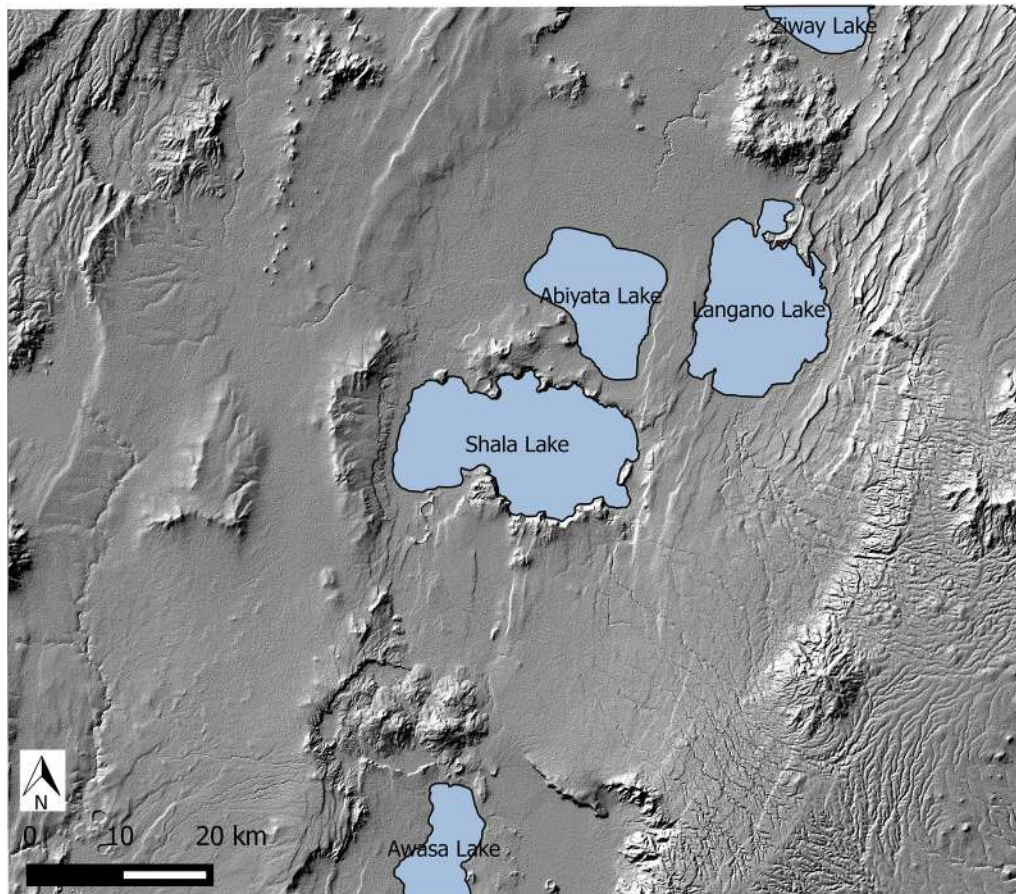


Fig. 4. Shaded DEM of the study area (about 10,640 km², ground resolution: 1 point every 50 m).

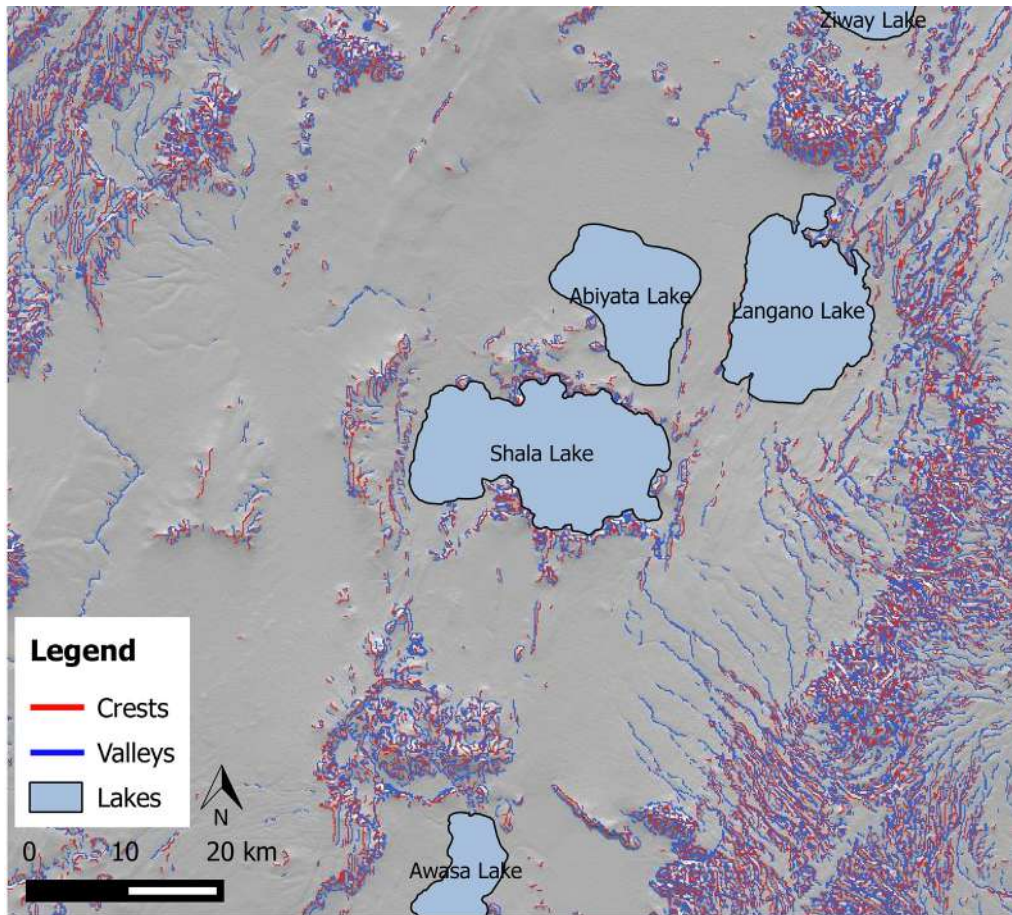


Fig. 5. Crests (red) and valleys (blue) identified by CurvaTool on the DEM of the study area.

lineament can be geometrically identified as a convex or concave edge of a DEM, particularly where there is structural control of the geomorphological evolution of the analyzed area. A detailed

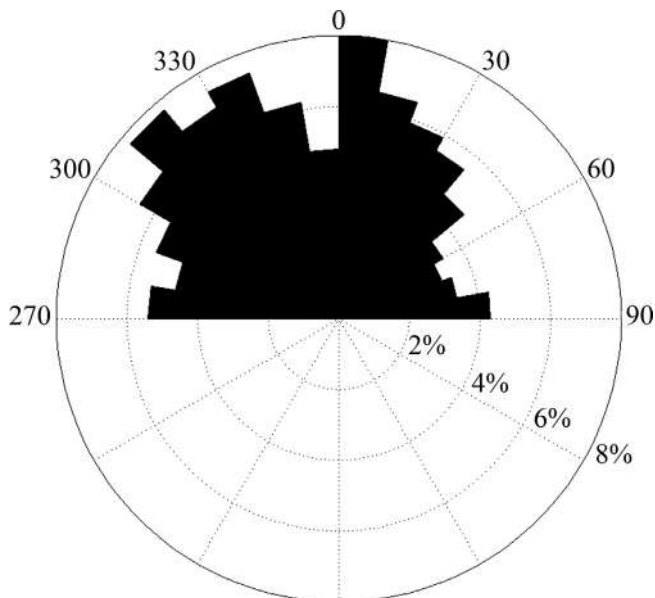


Fig. 6. Rosette diagram representing azimuthal frequencies (expressed as percentages of the total number of extracted linear features). Only the upper hemisphere is considered, since diametrically opposed directions are equivalent.

description of the working principles and calculation methods of CurvaTool code can be found in Bonetto et al. (2015b). This method works particularly well on models with a wide range of principal curvature values, namely on surfaces with a high degree of non-planarity. Therefore, quality and resolution of the DEM are fundamental in order to prevent smoothing effects that could compromise the effectiveness of this method (Bonetto et al., 2017). In the following, results from DEM processing will be illustrated and a test for investigating smoothing effect will be discussed.

The previously mentioned 30 m SRTM v3 DEM (Fig. 4) containing the study area (about 10,640 km²) was used as input for CurvaTool code; for computational issues its ground resolution was degraded to 1 point every 50 m. The area is mountainous, with an elevation difference of 1674 m, and the DEM surface is detailed enough to show a large number of recognizable crests and valleys. After CurvaTool processing, crests and valleys were identified (Fig. 5). Based on the rosette diagram (Fig. 6) obtained from the database produced by CurvaTool, three main azimuthal directions were identified (Table 1) and assigned to Filter code in order to perform a cluster analysis. After the application of Filter, linear fea-

Table 1
Orientation of lineament sets used as input for Filter.

Id set	Main direction	Azimuthal Direction [deg]	Standard Deviation [deg]
L1	N-S	10	10
L2	NNE-SSW	30	9.99
L3	NW-SE	325	25

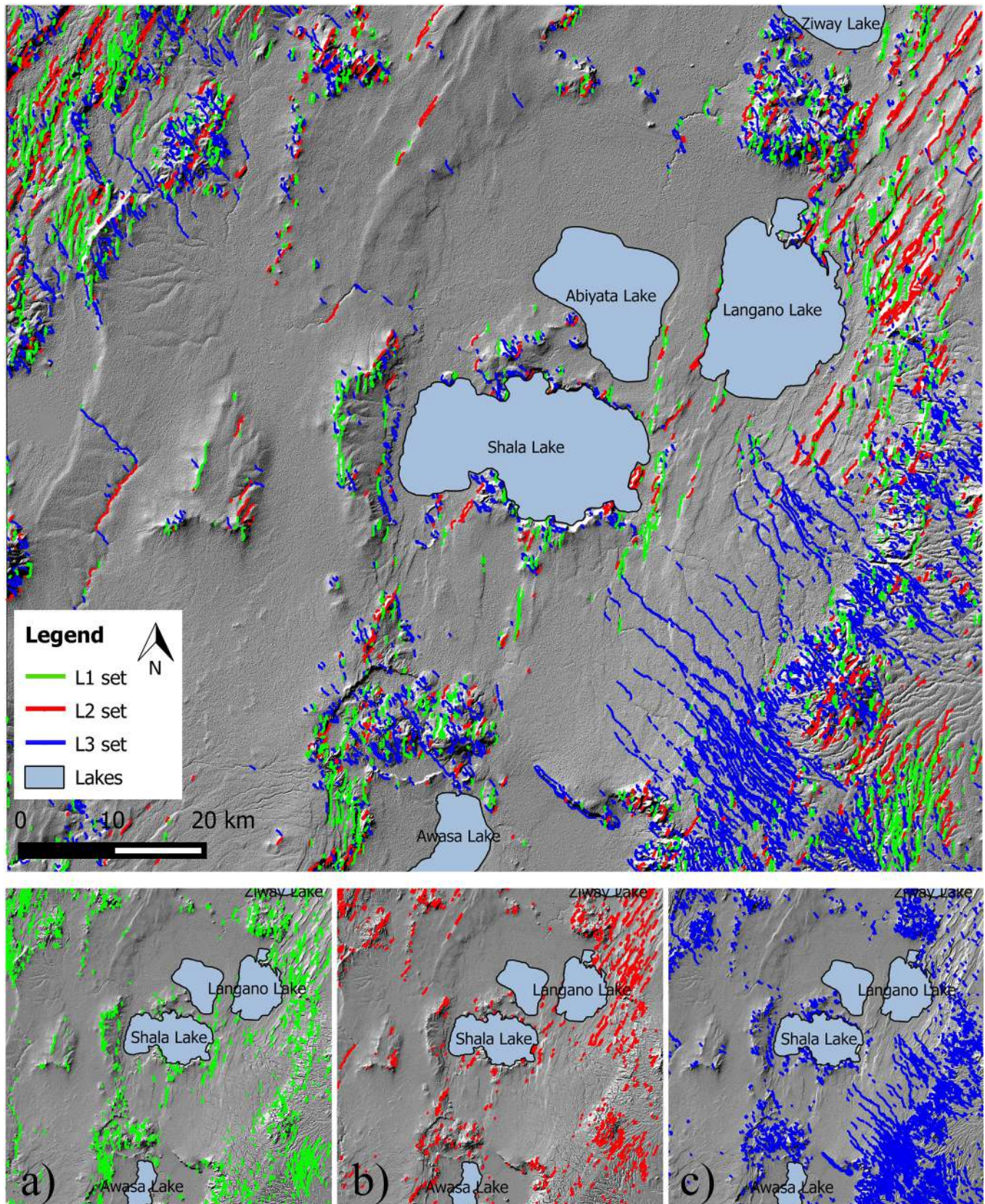


Fig. 7. Distribution of the three chosen sets in the whole area (Set L1, green; Set L2, red; Set L3, blue). Distribution of the single sets in the study area: a) L1, b) L2, c) L3.

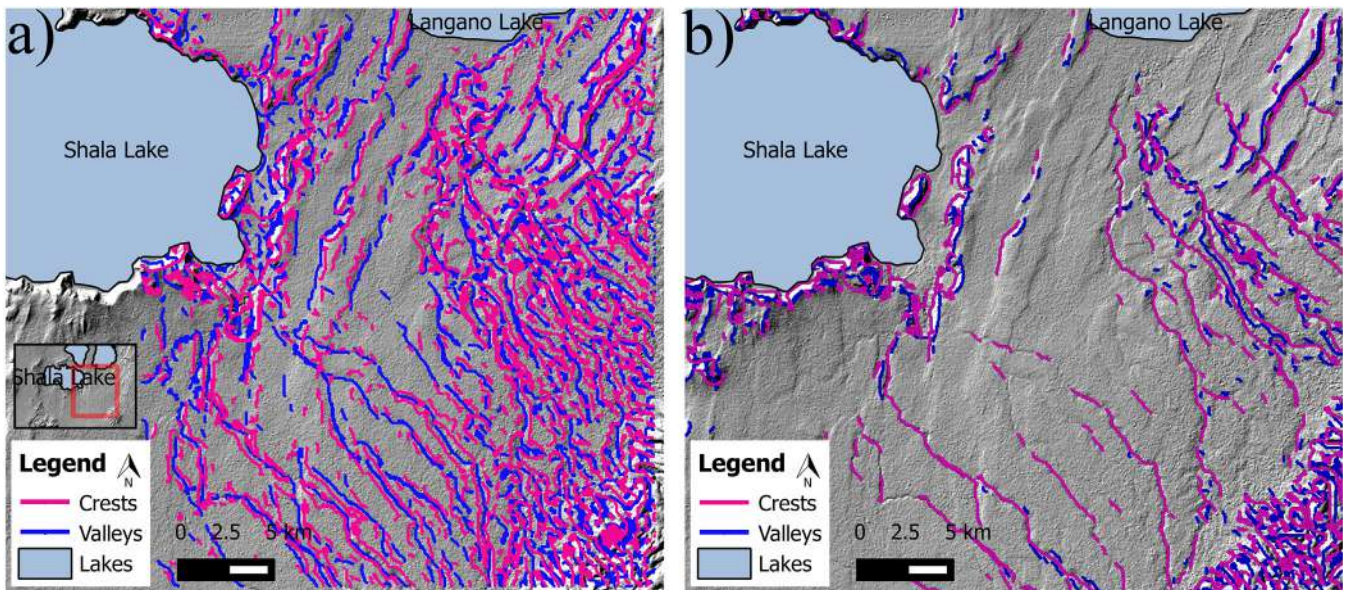


Fig. 8. a) Position of DEM Zoom (about 893 km², ground resolution: 1 point every 30 m) with respect of the original DEM; crests (purple) and valleys (blue) identified by CurvaTool on DEM Zoom. b) crests and valleys identified during the first processing.

tures belonging to the different sets were automatically represented in distinct colors (Fig. 7).

A portion of the original DEM was selected in order to analyze in detail its morphological features: this new DEM, called “DEM Zoom” in the following, covers an area of about 893 km², with an elevation difference of 1495 m and its ground resolution is the original one (1 point every 30 m). Similarly to what previously done for the DEM of the whole study area, CurvaTool produced a database of crests and valleys (Fig. 8).

Since the “DEM zoom” area (Fig. 8) was previously occupied by an ancient lake (those Langano, Abiyata and Shala lakes are the remnants) and it is now covered by lacustrine, fluvial and colluvial deposits, linear elements in this area are conditioned by water

extent variations and atmospheric agents, which model the sediments, more than tectonics. For this reason, the rosette diagram of Fig. 9 reports an azimuthal frequency distribution which is not directly linked to the tectonic asset of the region; therefore, the azimuthal directions applied in the Filter code (Table 1) are those derived by the rosette diagram of the entire area (Fig. 6), where volcanic rocks are present and tectonics has a strong control on the morphological features.

After the cluster analysis, linear features belonging to the different sets were automatically represented in distinct colors (Fig. 10).

4.1. Smoothing effect

The effect of the variation of the DEM resolution was investigated in order to better understand its influence on maximum and minimum principal curvature values, which are the main parameters calculated by CurvaTool and used in order to discriminate significant points belonging to crests and valleys. In particular, the study was focused on the decreasing of the resolution of the DEM, namely the increasing of the mean distance between adjacent points.

The previously described DEM Zoom was used for this purpose: the DEM was processed by means of CloudCompare V2.6 [<http://www.cloudcompare.org/>]. Subsample function was applied to vary the minimum distance between adjacent points, without modifying the size of the DEM: the characteristics of the subsampled DEMs are reported in Table 2.

The first effect of the decreasing of the resolution is the reduction of the number of points describing the surface: this influences particularly the elements characterized by a curve surface, such as crests (Fig. 11) and valleys (Fig. 12). Since the DEM is a discretized surface, the cross section of a curve element is a polyline made of a series of segments. Therefore, by progressively increasing the distance along the abscissa among points of a cross section, the resulting discretized curves differ from the original one not only in the number of points, but mainly in the slope and length of the segments.

Considering the whole DEM, the decreasing of resolution produces larger triangles, progressively less adherent to the real terrain surface. CurvaTool code implements curvature calculation

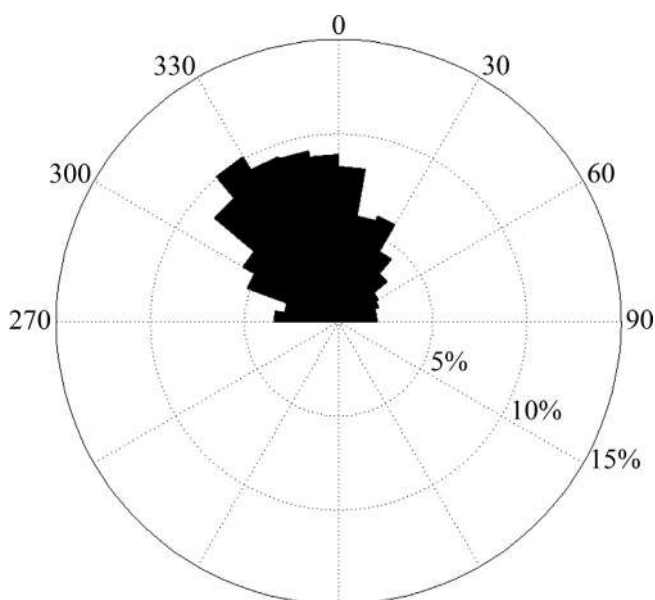


Fig. 9. Rosette diagram representing azimuthal frequencies (expressed as percentages of the total number of extracted linear features) obtained for DEM Zoom. Only the upper hemisphere is considered, since diametrically opposed directions are equivalent.

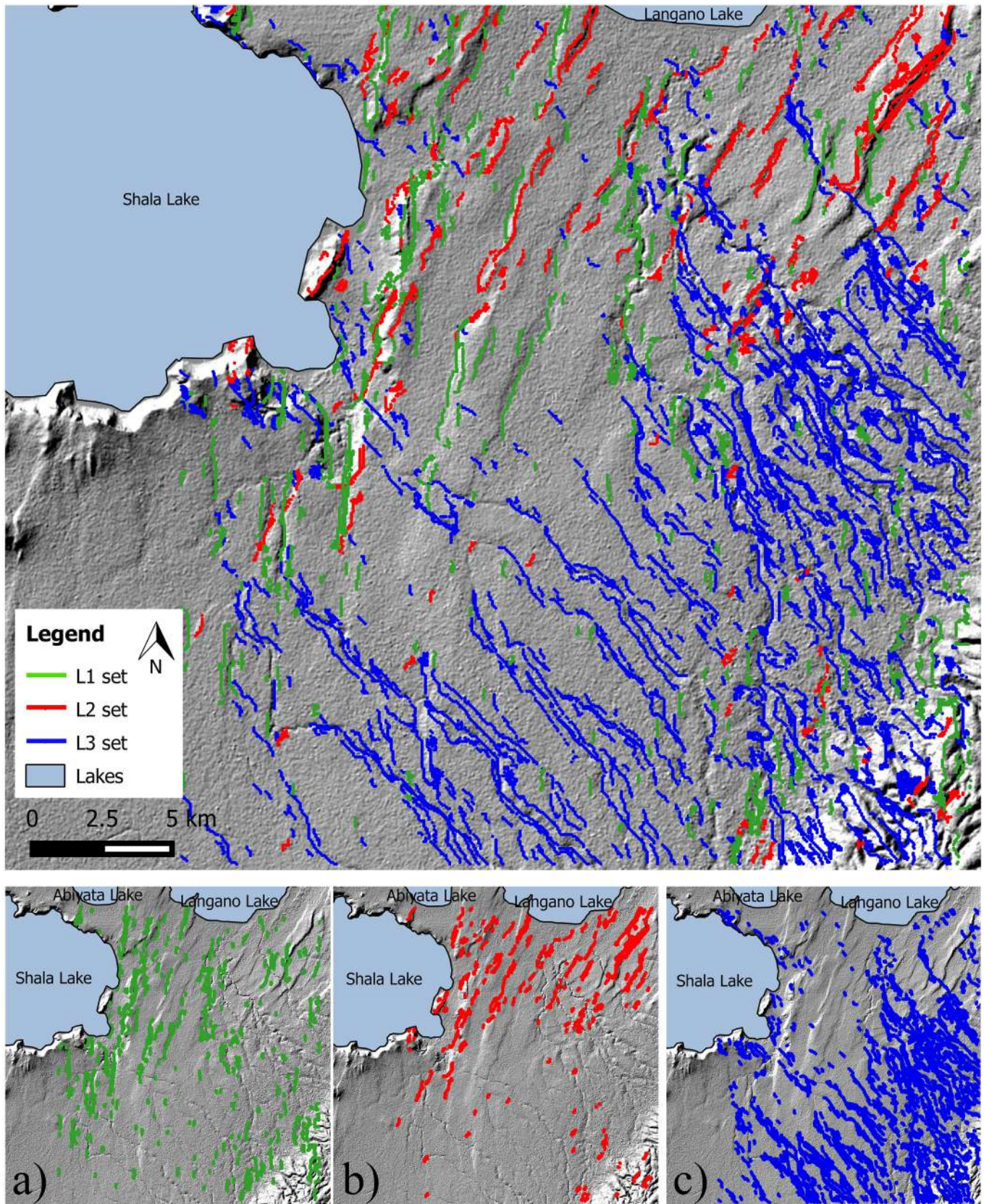


Fig. 10. Distribution of the three chosen sets in DEM Zoom area (Set L1, green; Set L2, red; Set L3, blue). Distribution of the single sets in the DEM Zoom area: a) L1, b) L2, c) L3.

Table 2
Resolution, number of points and triangles of the original and sub sampled DEMs.

Resolution [m]	N° of points	N° of triangles
30 (original)	948,738	1,893,576
40	474,323	946,696
50	237,418	473,088
90	105,647	210,086

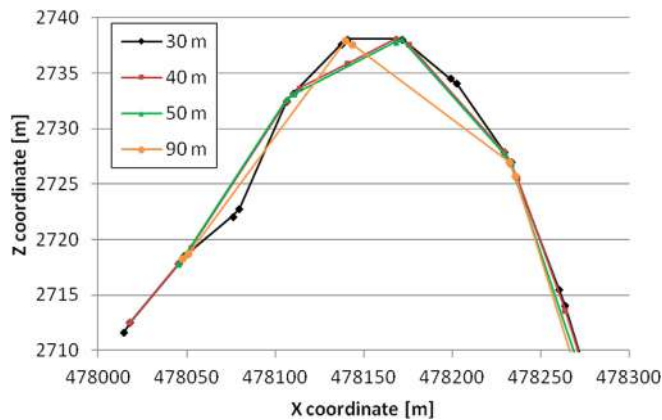


Fig. 11. Variation of a crest cross section due to the decreasing resolution.

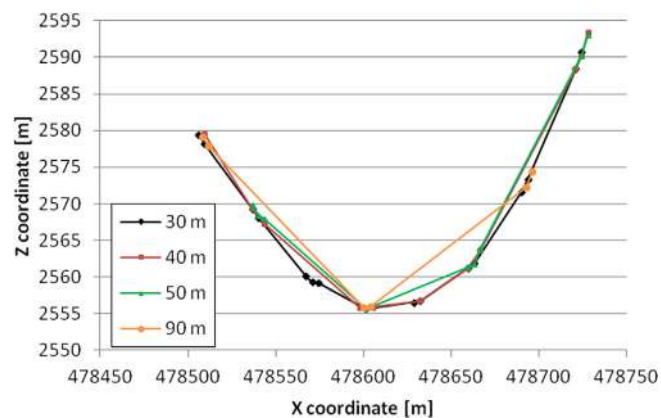


Fig. 12. Variation of a valley cross section due to the decreasing resolution.

for each point of the DEM: the method proposed by [Chen and Schmitt \(1992\)](#) is used. This method considers a two-ring neighborhood around each point. For each point, maximum (k_{max}) and minimum (k_{min}) principal curvature values are calculated. The greatest absolute value (minimum principal curvature is negative) indicates if the point belongs to a convex ($k_{max} > |k_{min}|$) or concave ($k_{max} < |k_{min}|$) portion of the surface of the DEM.

[Fig. 13](#) shows the frequency distributions of maximum and minimum principal curvature of the points of the DEM (in red those of the original DEM Zoom). First of all it must be noticed that the two frequency distributions and, in particular, the areas under them are different: this is due to the morphology of the DEM itself and it means that, in this case, the convex portion of DEM surface is predominant on the concave one. By reducing the resolution, the absolute values of k_{max} and k_{min} of the points decrease and distributions tend to become vertical, therefore values tend to become uniform: this can be called smoothing effect. It influences directly the number, length and continuity of linear elements identifiable by CurvaTool: in [Table 3](#) the comparison in terms of total length

of crest and valleys among the original and sub sampled DEMs is reported.

5. Discussion

Linear features identified by CurvaTool in the studied area are characterized by a non-homogeneous distribution. As shown in [Fig. 14](#), linear features are concentrated in the eastern and north-western sectors of the area. That distribution corresponds to the physiographic domains of the plateau and rift floor ([Boccaletti et al., 1999](#); [Benvenuti et al., 2002](#); [Abbate et al., 2015](#)). In the rift floor a few linear features were detected, particularly in correspondence of volcanic complexes (orange circles) or ancient and actual borders of the lakes. The margins of the rifts appear well defined by the concentration and the iso-orientation of linear features, which point out the presence of a nearly continuous system of faults, as confirmed by literature data ([Abebe et al., 1998](#); [Benvenuti et al., 2002](#); [Boccaletti et al., 1998](#)). Azimuthal frequencies represented in the rosette diagram ([Fig. 6](#)) and the consequent sets of linear features identified and used in Filter operations ([Table 1](#)) are congruent to the trend and distribution of the main fault systems reported in literature.

Set L1 is mainly recognized in the western plateau, in the Quaternary volcanic complex and in the rift floor, where the N-S to N20°E-trending fault system of the WFB is reported ([Boccaletti et al., 1998](#); [Benvenuti et al., 2002](#)). Short and random L1 linear features are observed in the eastern plateau, except for a sector in the easternmost corner of the analyzed area ([Fig. 15](#)). Set L2 is particularly evident in the eastern plateau and along the borders of the rift ([Fig. 16](#)), exactly where literature refers N35°E – N40°E to N-S/N20° striking trend ([Boccaletti et al., 1998](#); [Benvenuti et al., 2002](#)).

Set L3 is mainly located in the eastern plateau and in correspondence of the Quaternary Volcanic centers ([Fig. 17](#)); in particular,

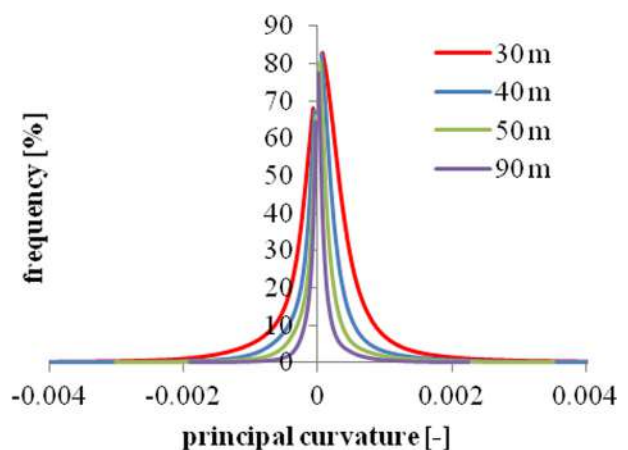


Fig. 13. Frequency distributions of maximum and minimum principal curvature of the points of the original and sub sampled DEMs.

Table 3
Comparison among total length of crests and valleys extracted by CurvaTool from the original and sub sampled DEMs.

Resolution [m]	Total length of crests [km]	Total length of valleys [km]
30 (original)	98.6	99.1
40	59.2	57.8
50	40.4	39.8
90	27.5	28.0

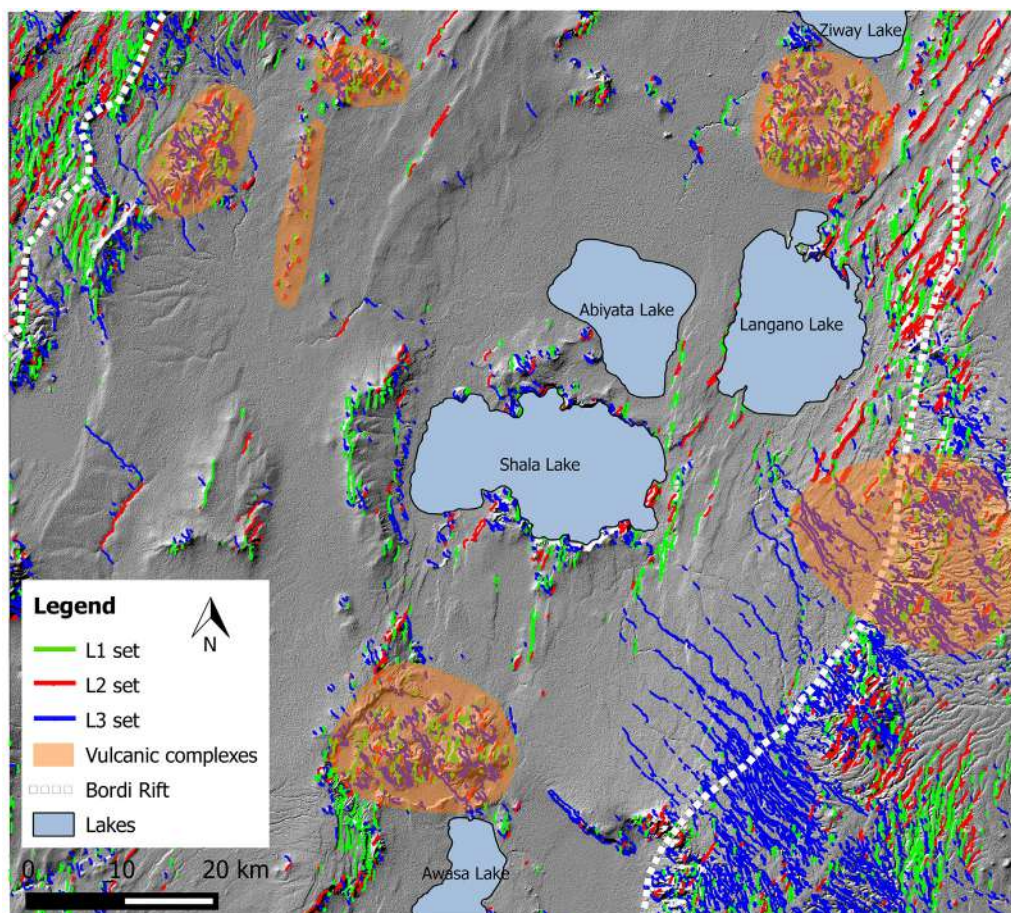


Fig. 14. Distribution of linear features, generated by CurvaTool processing, in the studied area.

along the eastern margin of the rift, NW-SE trending linear features cut the continuity of NE-SW linear features of the rift border, as reported by Boccaletti et al. (1998) and Benvenuti et al. (2002).

The obtained linear features distribution on DEM Zoom area confirms what underlined for the entire area, showing a concentration of sets L1 and L2 in the rift floor sector, whereas L3 is mainly identified along the eastern margin (Fig. 14).

Superimposing the distribution of water points censused in 2009 on the map with CurvaTool linear features database, it is possible to find a relationship between the types of water points (springs, hand-dug wells and deep wells) and areas with different linear features trends. Most of the censused water points are located in the eastern part of the studied area, where linear features are abundant. In particular, it is possible to note that the concentration of hand-dug wells and springs in the eastern marginal area of the rift corresponds to the area where set L3 was recognized. Instead, deep wells are mainly distributed in the rift floor, with particular regard to the sectors in which L1 and L2 represent the most frequent orientations (Figs. 18 and 19). Moreover, most water points are aligned coherently with the trend of linear features that CurvaTool identified in the area. This correspondence might highlight a likely matching with the potential groundwater flows paths and the structural linear features.

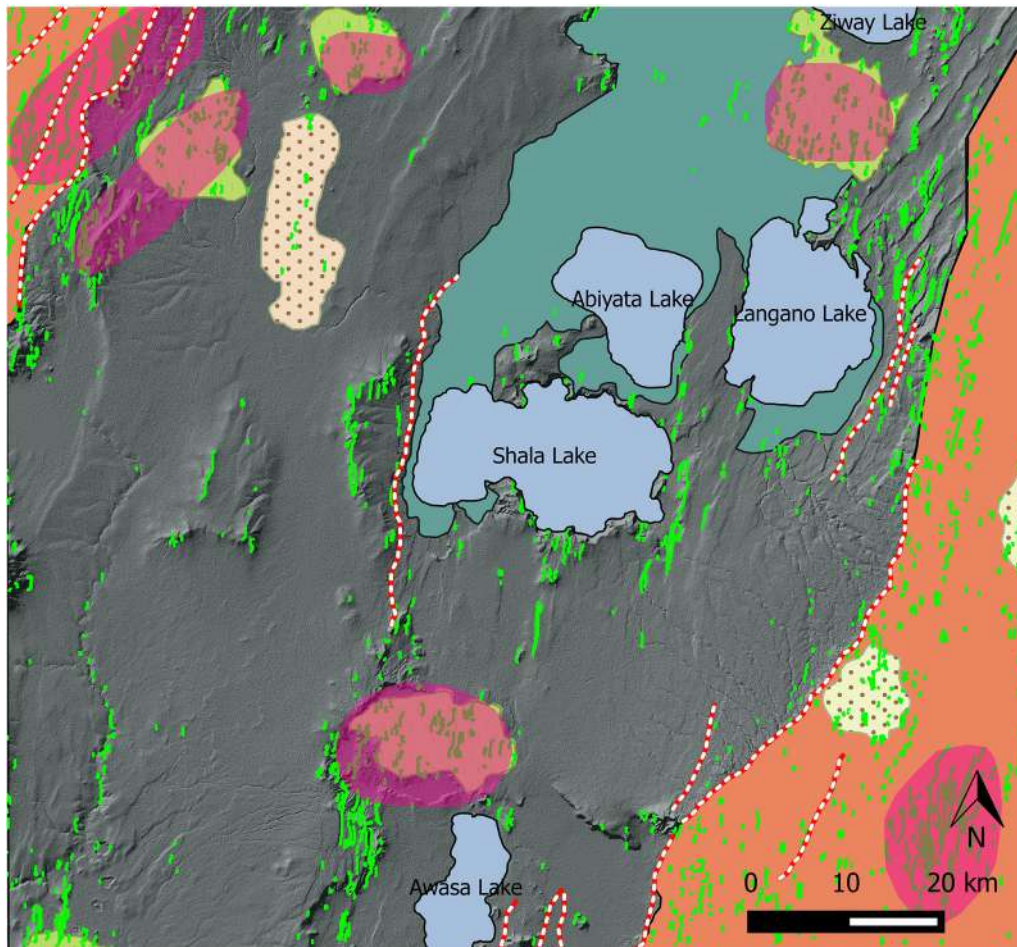
The coexistence of springs and hand-dug wells (indicating a shallow water level) with a dense net of crests and valleys with a specific trend (L3) along the southeastern escarpment suggests the existence of weathered or highly fractured rocks that are easier

to model (abundance of crests and valleys), probably tectonically controlled (iso-orientation of the linear features), which represent a permeable continuous and shallow aquifer (abundance of superficial water points). The censused springs and hand-dug wells show alignment coherent with the orientation of linear features belonging to L3, which, in turn, are coherent with the structural trend reported in literature (Benvenuti et al., 2002).

In the rift floor, the lower number of iso-oriented morphological linear features detected by CurvaTool and the prevalence of deep wells, mainly distributed along the same direction of the detected linear features, suggest the presence of a main fractured unconfined aquifer, represented by volcanic rocks locally affected by faults (L1 and L2), which act as main path for water flow.

6. Conclusions

A semi-automatic approach (CurvaTool) was applied to analyze geological lineaments in an area of CMER to better understand the role of potential structural elements in local water distribution. A first processing was carried out over the whole area. From this analysis, a problem linked to the morphological features in a rift sector was revealed. Indeed, due to the scarce differences in height, the thresholds assumed in the first processing were not adequate to highlight linear features in the rift floor. Therefore, a second processing was carried out over a significant portion of the original DEM (DEM Zoom).



Geology





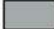




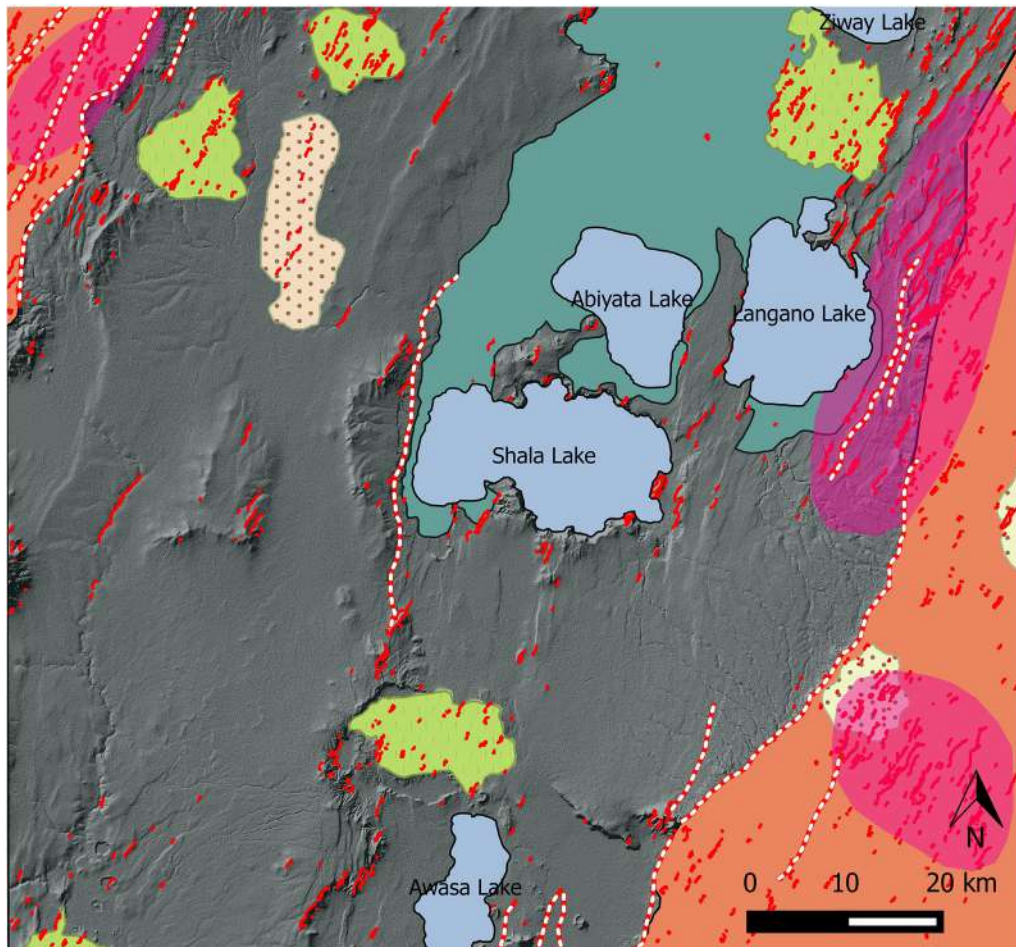
 Lacustrine, fluvial and colluvial deposits	 Main Fault
 Volcanites of the plateau	 Lakes
 Rift floor ignimbrites	 L1 set
 Rhyolitic lava flow	
 Basaltic lava flows and scoria cones	
 Basalts, mugearites, trachytes and phonolites	

Fig. 15. Distribution of L1 set. Pink circles identify sectors where L1 is mainly recognized.

The tectono-metamorphic information inferred by the processing, both on the whole area and on DEM Zoom, agree with geological and structural literature data and contribute to identify the three major physiographic regions (rift floor, escarpment and highlands) that condition the hydrogeological setup.

Linear features sets L1 and L2 are coherent with the main structural trend associated to the opening of the rift and correspond to the regional geological asset of the whole MER, including the studied area. The presence of set L3 is confirmed by data reported in the detailed geological map of Zway-Shala basin (Benvenuti et al., 2002), suggesting the presence of a NW-SE trending fault system in the same sector in which CurvaTool indicates this trend. These results contribute to validate the significance of CurvaTool output and the potentiality of this method for a preliminary and fast detection of topographical and morphological elements. A correla-

tion between the distribution of productive water points censured in the area and linear features detected by CurvaTool has been highlighted. Most of the water points show alignments coherent with CurvaTool linear features and suggest the presence of different aquifers, highlighted by the concentration of deep wells in correspondence of rift floor sectors, marked by L1 and L2 linear trends, and of springs and hand-dug wells along escarpments, characterized by L3 linear trend. This remark is coherent with the general hydrogeological model of the rift proposed by different authors (Ayenew et al., 2008; EIGS, 1993; Rango et al., 2010), in which groundwater flows from the highlands to the rift floor, where flow is controlled by a series of normal faults mainly oriented along the NE-SW Rift axis; moreover, the presence of marginal faults along escarpments favors the formation of high discharge and fault controlled springs.



Geology





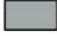




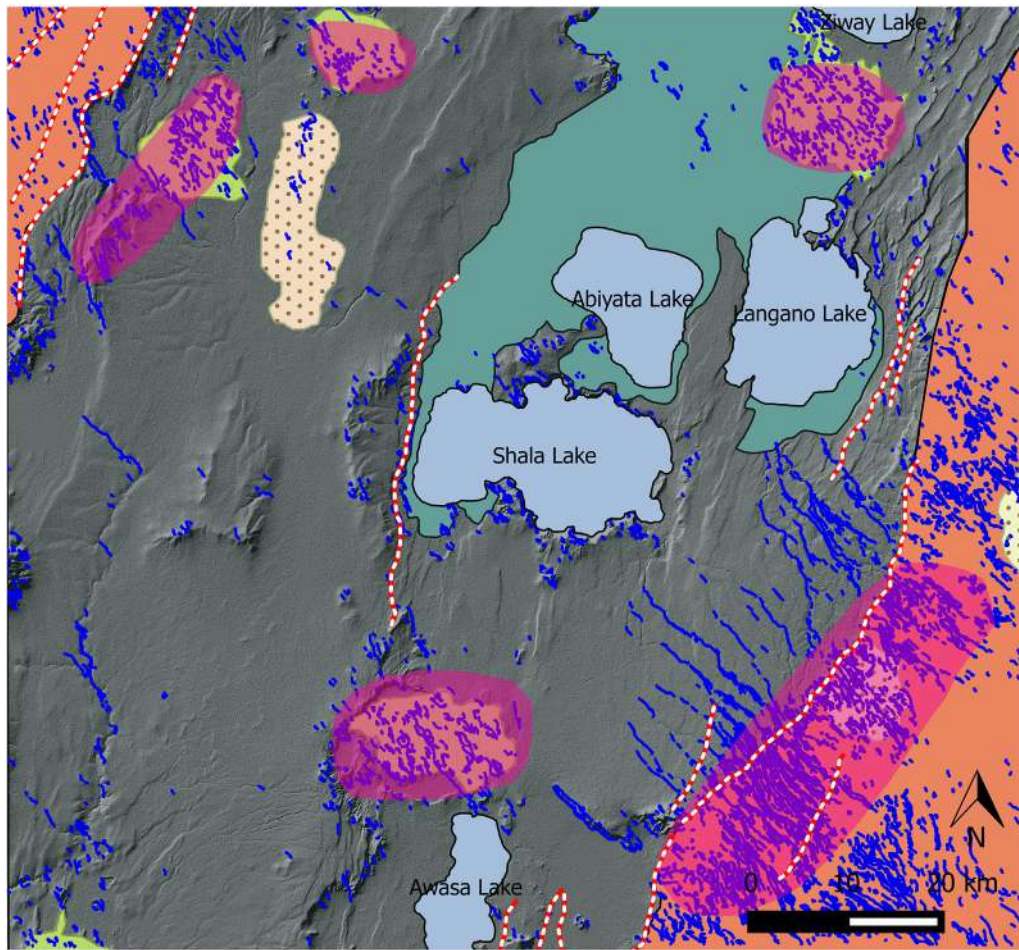
- | | | | |
|---|---|--|------------|
|  | Lacustrin, fluvial and colluvial deposits |  | Main Fault |
|  | Volcanites of the plateau |  | Lakes |
|  | Rift floor ignimbrites |  | L2 set |
|  | Rhyolitic lava flow | | |
|  | Basaltic lava flows and scoria cones | | |
|  | Basalts, mugearites, trachytes and phonolites | | |

Fig. 16. Distribution of set L2; pink circles identify sectors where L2 is mainly recognized.



Geology





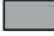




- | | | | |
|---|---|--|------------|
|  | Lacustrin, fluvial and colluvial deposits |  | Main Fault |
|  | Volcanites of the plateau |  | Lakes |
|  | Rift floor ignimbrites |  | L3 set |
|  | Rhyolitic lava flow | | |
|  | Basaltic lava flows and scoria cones | | |
|  | Basalts, mugearites, trachytes and phonolites | | |

Fig. 17. Distribution of set L3; pink circles identify sectors where L3 is mainly recognized.

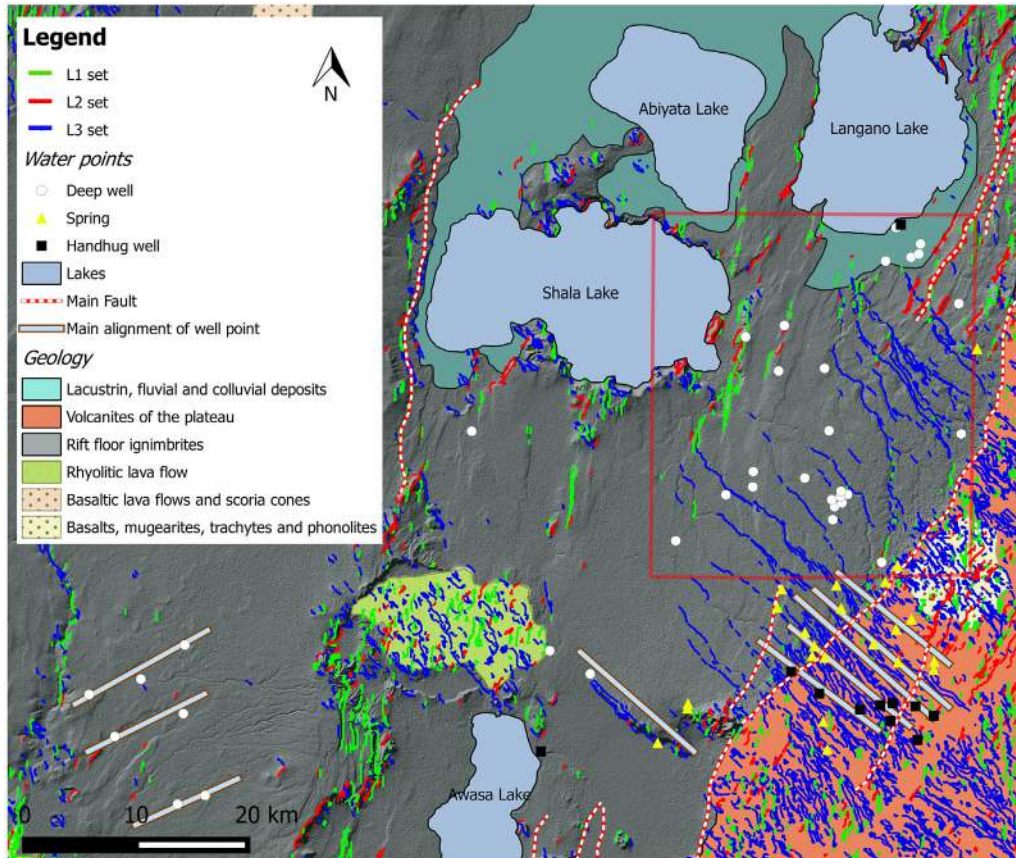


Fig. 18. Distribution of water points and CurvaTool linear features in the studied area. Red frame includes DEM Zoom, analyzed in detail in Fig. 19.

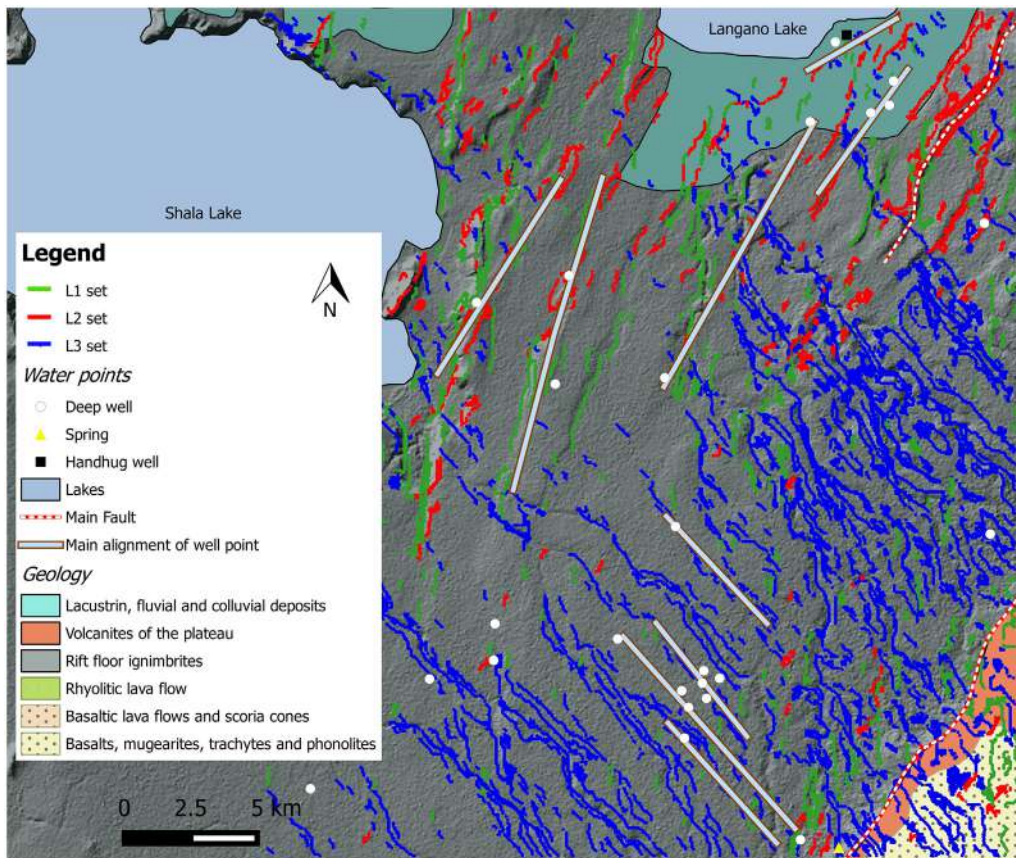


Fig. 19. Distribution of water points and CurvaTool linear features in DEM Zoom area.

The first results obtained in this study suggest the reliability of CurvaTool and its usefulness in preliminary structural and hydrogeological studies, particularly in areas where groundwater flow is strongly conditioned by topography and morphotectonic asset or in case of lack of geological information.

The development and application of such methodologies could help and support hydrogeological researches aiming to assure the access to safe drinking water to people living in areas where field investigations and accessibility are difficult.

Conflict of interest

None declared.

References

- Abbate, E., Bruni, P., Painossa Sagri, M., 2015. Geology of Ethiopia: a review and geomorphological perspectives. In: Billi, P. (Ed.), *Landscapes and Landforms of Ethiopia*. Springer, Dordrecht, The Netherlands, pp. 32–64.
- Abebe, B., Boccaletti, M., Mazzuoli, R., Bonini, M., Tortorici, L., Trua, T., 1998. Geological map of the Lake Ziway-Asela region (Main Ethiopian Rift). 1:50,000 scale. C.N.R., ARCA, Firenze, Italy.
- Adeyemi, A.J., 2016. Current status on the use of remote sensing and GIS techniques for groundwater mapping in Nigeria. *Achiev. J. Sci. Res.* 1 (2), 105–119.
- Akame, J.M., Mvondo Ondo, J., Teikeu, A.W., Owona, S., Olinga, J.B., Messi Ottou, E.J., Ntomba, S., 2014. Apport des Images Landsat-7 ETM+ a l'etude structurale du socle archeen de sangmelima (Sud Cameroun). *Rev. Fr. Photograph. Télédélect.* 206, 15–26.
- Anudu, G.K., Essien, B.I., Onuba, L.N., Ipkokonte, A.E., 2011. Lineament analysis and interpretation for assessment of groundwater potential of Wamba and adjoining areas, Nasarawa State, north-central Nigeria. *J. Appl. Technol. Environ. Sanit.* 1 (2), 185–192.
- Assatse, W.T., Nouck, P.N., Tabod, C.T., Akame, J.M., Biriganine, G.N., 2016. Hydrogeological activity of lineaments in Yaoundé Cameroon region using remote sensing and GIS techniques. *Egypt J. Remote Sens. Space Sci.* 19 (1), 49–60.
- Aynew, T., 2008. The distribution and hydrogeological controls of fluoride in the groundwater of central Ethiopian rift and adjacent highlands. *Environ. Geol.* 54, 1313–1324.
- Aynew, T., Demlie, M., Wöhnlich, S., 2008. Hydrogeological framework and occurrence of groundwater in the Ethiopian aquifers. *J. Afr. Earth Sci.* 52, 97–113.
- Benvenuti, M., Carnicelli, S., Belluomini, G., Dainelli, N., Di Grazia, S., Ferrari, G.A., Iasio, C., Sagri, M., Ventra, D., Balemwald, A., Kebede, S., 2002. The Ziway-Shala lake basin (main Ethiopian rift, Ethiopia): a revision of basin evolution with special reference to the Late Quaternary. *J. Afr. Earth Sci.* 35 (2), 247–269.
- Boccaletti, M., Bonini, M., Mazzuoli, R., Abebe, B., Piccardi, L., Tortici, L., 1998. Quaternary oblique extensional tectonics in the Ethiopian Rift (Horn of Africa). *Tectonophysics* 287, 97–116.
- Boccaletti, M., Bonini, M., Mazzuoli, R., Trua, T., 1999. Pliocene-Quaternary volcanism and faulting in the northern Main Ethiopian Rift (with two geological maps at scale 1:50,000). *Acta Vulcanol.* 11 (1), 83–97.
- Bonetto, S., Facello, A., Cristofori, E.I., Camaro, W., Demarchi, A., 2016. An approach to use Earth observation data as support to water management issues in the Ethiopian rift. *Symposium on Climate Change Adaptation in Africa 2016 – Addis Ababa, Ethiopia*.
- Bonetto, S., De Luca, D., Lasagna, M., Lodi, R., 2015a. Groundwater distribution and fluoride content in the West Arsi Zone of the Oromia Region (Ethiopia). In: Lollino (Ed.), *Engineering Geology for Society and Territory*, vol. 3: River Basins, Reservoir Sedimentation and Water Resources. Springer, Torino, pp. 579–582.
- Bonetto, S., Facello, A., Ferrero, A.M., Umili, G., 2015b. A tool for semi-automatic linear feature detection based on DTM. *Comput. Geosci.* 75, 1–12.
- Bonetto, S., Facello, A., Umili, G., 2017. A new application of CurvaTool semi-automatic approach to qualitatively detect geological lineaments. *Environ. Eng. Geosci.* 23 (3), 179–190.
- Chen, X., Schmitt, F., 1992. Intrinsic Surface Properties from Surface Triangulation. *Proceedings of the European Conference on Computer Vision*, pp. 739–743.
- Chuma, C., Orimogunje, O.I., Hlatywayo, D.J., Akinyede, J.O., 2013. Application of remote sensing and geographical information systems in determining the groundwater potential in the crystalline basement of Bulawayo metropolitan Area, Zimbabwe. *J. Adv. Remote Sens.* 2, 149–161.
- Corgne, S., Magagi, R., Yergeau, M., Sylla, D., 2010. An integrated approach to hydrogeological lineament mapping of a semi-arid region of West Africa using Radarsat-1 and GIS. *Remote Sens. Environ.* 114 (9), 1863–1875.
- Edet, A.E., Okereke, C.S., Teme, S.C., Esu, E.O., 1998. Application of remote-sensing data to groundwater exploration: a case study of the Cross River State, southeastern Nigeria. *Hydrogeol. J.* 6 (3), 394–404.
- EIGS, 1993. Hydrogeological Map of Ethiopia. 1:2,000,000 Scale. Ethiopian Institute of Geological Surveys, Addis Ababa.
- El-Naqa, A., Hammouri, N., Ibrahim, K., El-Taj, M., 2009. Integrated approach for groundwater exploration in Wadi Araba using remote sensing and GIS. *Jordan J. Civ. Eng.* 3 (3), 229–243.
- Fernandes, A.J., Rudolph, D.L., 2001. The influence of Cenozoic tectonics on the groundwater production capacity of fractured zones: a case study in Sao Paulo, Brazil. *Hydrogeol. J.* 9, 151–167.
- Elewa, H.H., Qaddah, A.A., 2011. Groundwater potentiality mapping in the Sinai Peninsula, Egypt, using remote sensing and GIS-watershed-based modelling. *Hydrogeol. J.* 19 (3), 613–628.
- Jacques, P.D., Machado, R., Nummer, A.R., 2012. A comparison for a multiscale study of structural lineaments in southern Brazil: LANDSAT-7 ETM+ and shaded relief images from SRTM3-DEM. *Anais Acad. Brasileira Ciências* 84 (4), 931–942.
- Keranen, K., Klemperer, S.L., 2008. Discontinuous and diachronous evolution of the Main Ethiopian Rift: implications for development of continental rifts. *Earth Planet Sci. Lett.* 265, 96–111.
- Luczaj, J., 2016. Groundwater quantity and quality. *Resources* 5 (10), 1–4.
- Mabee, S.B., Hardcastle, K.C., Wise, D.U., 1994. A method of collecting and analyzing lineaments for regional-scale fractured-bedrock aquifer studies. *Groundwater* 32 (6), 884–894.
- Magaiia, L.A., Goto, T., Masoud, A.A., Koike, K., 2017. Identifying groundwater potential in crystalline basement rocks using remote sensing and electromagnetic sounding techniques in Central Western Mozambique. *Nat. Resour. Res.* <https://doi.org/10.1007/s11053-017-9360-5>.
- Magowe, M., Carr, J.R., 1999. Relationship between lineaments and ground water occurrence in western Botswana. *Groundwater* 37 (2), 282–286.
- Masoud, A., Koike, K., 2006. Tectonic architecture through Landsat-7 ETM+/SRTM DEM-derived lineaments and relationship to the hydrogeologic setting in Siwa region, NW Egypt. *J. Afr. Earth Sci.* 45, 467–477.
- Mogaji, K.A., Aboyeji, O.S., Omosuyi, G.O., 2011. Mapping of lineaments for groundwater targeting in the basement complex region of Ondo State, Nigeria, using remote sensing and geographic information system (GIS) techniques. *Int. J. Water Resour. Environ. Eng.* 3 (7), 150–160.
- Obiefuna, G.I., Adamolekun, S.S., Ishaku, J.M., 2010. Determining potential areas of groundwater occurrences using remote sensing techniques: a case study of Mubi area, Northeast, Nigeria. *Cont. J. Appl. Sci.* 5, 15–24.
- Okereke, C.N., Ikoru, D.O., Amadi, C., Okorafor, O.O., 2015. Groundwater accessibility using remote sensing technique: a case study of Orlu and Adjoining areas, Southeastern Nigeria. *Sci. Res. J.* 3 (3), 12–20.
- Phukon, P., Chetia, D., Laskar, A.A., 2012. Application of remote sensing and geographic information system for groundwater resource mapping: a preliminary appraisal in Guwahati City, Assam. *Int. J. Comp. Appl. Eng. Sci.* 2 (2), 107–113.
- Prabu, P., Rajagopalan, B., 2013. Mapping of lineaments for groundwater targeting and sustainable water resource management in hard rock hydrogeological environment using RS-GIS. In: Ray, Pallav (Ed.), *Climate Change and Regional/Local Responses*. InTech, pp. 235–247.
- Rango, T., Bianchini, G., Beccaluva, L., Tassinari, R., 2010. Geochemistry and water quality assessment of central Main Ethiopian Rift natural waters with emphasis on source and occurrence of fluoride and arsenic. *J. Afr. Earth Sci.* 57, 479–491.
- Rashid, M., Lone, M.A., Ahmed, S., 2012. Integrating geospatial and ground geophysical information as guidelines for groundwater potential zones in hard rock terrains of south India. *Environ. Monit. Assess.* 184 (8), 4829–4839.
- Singh, P., Thakur, K.J., Kumar, S., 2013. Delineating groundwater potential zones in a hard-rock terrain using geospatial tool. *Hydrol. Sci. J.* 58 (1), 213–223.
- Sultan, M., Wagdy, A., Manocha, N., Sauck, W., Abdel Gelil, K., Youssef, A.F., Becker, R., Milewski, A., El Alfy, Z., Jones, C., 2008. An integrated approach for identifying aquifers in transcurrent fault systems: the Najd shear system of the Arabian Nubian shield. *J. Hydrol.* 349 (3–4), 475–488.
- Talab, A.O., Tijani, M.N., 2011. Integrated remote sensing and GIS approach to groundwater potential assessment in the basement terrain of Ekiti area southwestern Nigeria. *RMZ Mater. Geoenviron.* 58 (3), 303–328.
- Tesemma, A., Mengistu, H., Chirenje, E., Abiye, T.A., Demlie, M.B., 2012. The relationship between lineaments and borehole yield in North West Province, South Africa: results from geophysical studies. *Hydrogeol. J.* 20 (2), 351–368.
- Umili, G., Ferrero, A.M., Einstein, H.H., 2013. A new method for automatic discontinuity traces sampling on rock mass 3Dmodel. *Comput. Geosci.* 51, 182–192.
- Yenne, E.Y., Anifowose, A.Y.B., Dibal, H.U., Nimchak, R.N., 2015. An assessment of the relationship between lineament and groundwater productivity in a part of the basement complex, Southwestern Nigeria. *IOSR J. Environ. Sci. Toxicol. Food Technol.* 9 (6), 23–35.